The 9th European Congress on Computational Methods in Applied Sciences and Engineering
ECCOMAS Congress 2024
3–7 June 2024, Lisboa, Portugal

DESIGN OF AN AUXETIC AND STANDARD SOFT MATERIAL FOR ADDITIVE MANUFACTURING USING A HEURISTIC RBSM APPROACH

LUIS C.M. DA SILVA[1] AND SIRO CASOLO[1]

[1] Politecnico di Milano, Department A.B.C.
Piazza Leonardo da Vinci, 20133, Milan, Italy
e-mail: {luiscarlos.martinsdasilva, siro.casolo}@polimi.it

Key words: Heuristic molecule, auxetic, RBSM, Cosserat, Soft material

Summary. This study contributes to the field of additive manufacturing of metamaterials. Design examples are presented to create two very soft microstructures: an auxetic material ($\nu = -1.0$) and a standard material ($\nu = 0.2$) that share the same low shear modulus ($G = 5.0$ MPa), despite the use of a standard printing material. The design is based on a planar topology, with its unit-cell derived from a RBSM heuristic molecule (HM) composed of shaped atoms with both centered and non-centered spring-based interactions. A homogenization approach is employed to establish a relationship between the stiffness of these spring-bonds and the macroscopic elastic properties of a isotropic Cosserat material. The practical significance of the present HM lies in the fact that: (i) it is modelled through a continuum-based Finite Element model, and (ii) the constitutive description of atoms and bonds is determined based on the elastic properties of the material used in the printing process, combined with the topology. Results demonstrate a good match with the expected properties and a quasi-isotropic response, especially when the deformability of atoms is low.

1 INTRODUCTION

The development of novel metamaterials able to respond to various stimuli is supported by the progress in additive manufacturing processes [1]. Multi-functional composite materials, which exhibit diverse response mechanisms, can be designed by incorporating metals and polymers in complex geometries [1]. Special emphasis is herein placed on auxetic metamaterials, which are of significant interest due to their wide range of applications [2]. Noteworthy properties of these materials include enhanced responses to shear actions [3], indentation [4], and fracture [5], along with variable permeability [6] and improved energy absorption and impact capacity [7].

The use of a discrete approach to identify material geometries is currently explored in the design of metamaterials. Matlack et al. [8] developed a material with weakly interacting 2D unit cells, enabling the creation of Veselago lenses, zero-dispersion bands, and topological surface phonons. Wang et al. [9] utilized periodic and discrete 2D unit cells to evaluate the wave propagation properties of metamaterials. Given the limited practical engineering applicability of spring network-based models, the adoption of continuum Finite Element (FE) models may provide a more realistic numerical solution for additive manufacturing processes [10].

Within this context, the present study aims to extend the results from a rigid body spring model (RBSM) to a continuum Finite Element (FE) model. As recently demonstrated [10], the

RBSM is based on a heuristic molecule developed by the authors in previous studies [11, 12]. Initially, a topology is identified to exhibit specific mechanical characteristics of the material. Subsequently, sensitivity analyses are conducted, and the results from the FE model are discussed.

2 BOND-BASED HEURISTIC MOLECULAR MODEL

A bond-based model, based on the hypothesis of pair-potentials [13], supports the design of a two-dimensional topology that exhibits the desired mechanical properties, as presented in [11, 12]. A planar solid materials consists of a finite number of heuristic molecules (HM), which are made by atoms that possess mass and a specific polygonal shapes. These are significantly more rigid relative to the other components of the system. In the reference (undeformed) configuration, the atoms are disposed according to a structured lattice organization. A local condition is imposed such that only adjacent atoms interact via bonds characterized by a linear elastic potential through spring elements. The complete set of centered and non-centered bonds is illustrated in Fig. 1a. Axial bonds include cyan (horizontal and vertical) and red (diagonal) springs. Shear bonds, which are non-centered and orthogonal to the direction of the bonded atoms, are represented by magenta and green springs.

2.1 Linearized kinematics and elastic deformation energy

The kinematic mapping χ between a given reference (undeformed) configuration $\mathbf{X}$ and a deformed one $\overset{\star}{\mathbf{X}}$ is given as $\chi : \mathbf{X} \rightarrow \overset{\star}{\mathbf{X}}$. The relative Lagrangian displacements and rotations are given as $\mathbf{U} = \overset{\star}{\mathbf{X}} - \mathbf{X}$ and $\mathbf{\Psi} = \overset{\star}{\mathbf{\Phi}} - \mathbf{\Phi}$, respectively. For an arbitrary bond b, within the material domain Ω that links atoms i and j, the bond vector $\mathbf{d}_b$ is given in Eq. (1) and the deformed bond vector $\overset{\star}{\mathbf{d}}_b$ in Eq. (2).

$$\mathbf{d}_b = (\mathbf{x}^j + \mathbf{r}_b^j) - (\mathbf{x}^i + \mathbf{r}_b^i) \tag{1}$$

$$\overset{\star}{\mathbf{d}}_b = (\overset{\star}{\mathbf{x}}^j + \overset{\star}{\mathbf{r}}_b^j) - (\overset{\star}{\mathbf{x}}^i + \overset{\star}{\mathbf{r}}_b^i) \tag{2}$$

where $\mathbf{r}_b^i$ and $\mathbf{r}_b^j$ represent the rigid arms of the bond b with respect to atoms i and j, respectively. The vectors $\overset{\star}{\mathbf{r}}_b^i$ and $\overset{\star}{\mathbf{r}}_b^j$ denote the rigid arms of the atoms after the deformation of the bond b. The relative displacement vector of bond b, linking atoms i and j, is described as δ_b and is determined according to the global reference frame by $\delta_b = \overset{\star}{\mathbf{d}}_b - \mathbf{d}_b$. The interatomic bonds (Fig. 1a) experience simple axial deformations and resemble axial springs. The strain energy for an arbitrary bond b with stiffness k_b and direction $\boldsymbol{\xi}_b$ in the reference configuration has a quadratic dependence on the variation of the initial bond length:

$$\mathcal{U}_{b_\xi}(\boldsymbol{\delta}_b) = \frac{1}{2} k_b (\boldsymbol{\xi}_b \cdot \boldsymbol{\delta}_b)^2 \tag{3}$$

2.2 Relation with a reference continuum FE model

The HM topology, which will be used for the design of quasi-isotropic non-linear auxetic material, can be related with a Cosserat continuum. The constitutive response in isotropic linear elasticity is described by:

$$\left\{\begin{array}{c} S_{11} \\ S_{22} \\ S_{12} \\ S_{21} \\ M_{13} \\ M_{23} \end{array}\right\} = \left[\begin{array}{cccccc} \mathsf{C}_{1111} & \mathsf{C}_{1122} & 0 & 0 & 0 & 0 \\ \mathsf{C}_{1122} & \mathsf{C}_{2222} & 0 & 0 & 0 & 0 \\ 0 & 0 & G+G_c & G-G_c & 0 & 0 \\ 0 & 0 & G-G_c & G+G_c & 0 & 0 \\ 0 & 0 & 0 & 0 & 2Gd^2 & 0 \\ 0 & 0 & 0 & 0 & 0 & 2Gd^2 \end{array}\right] \left\{\begin{array}{c} E_{11} \\ E_{22} \\ E_{12} \\ E_{21} \\ K_{13} \\ K_{23} \end{array}\right\} \tag{4}$$

in which $\mathsf{C}_{1111} = \mathsf{C}_{2222} = \frac{2G}{1-\nu}$ and $\mathsf{C}_{1122} = \frac{2G\nu}{1-\nu}$ for a Plane-stress (PS) problem; the Cosserat shear modulus G_c governs the specific skew-symmetric contribution to the shear elastic response; and d is the internal characteristic length associated to in-plane bending. Through the equivalence of strain density energy between the HM and a plane-stress continuum, the stiffness of the bonds is determined. A total of five kinematic modes are considered: in-plane bending, and the micropolar, uniaxial, deviatoric, and hydrostatic modes [11, 12]. The bond stiffness is subsequently calculated based on these modes:

$$k_c^{\mathsf{PS}} = G\Big(\frac{d}{\|\mathbf{r}_c\|}\Big)^2 \quad , \quad k_r^{\mathsf{PS}} = G\frac{1+\nu}{1-\nu} - k_c \quad , \quad k_m^{\mathsf{PS}} = -2G\frac{\nu}{1-\nu} + k_c \tag{5}$$
$$k_g^{\mathsf{PS}} = G - k_c \quad , \quad G_c^{\mathsf{PS}} = \frac{1-3\nu}{1-\nu}G$$

3 MICROSTRUCTURE DESIGN AND FE CONTINUUM NUMERICAL MODELLING

The design of two microstructure is conducted in this section based on the same value of macroscopic shear modulus ($G = 5.0$ MPa), i.e. for: (1) a ultra-soft and auxetic material with $\nu = -1.0$, and (2) a very soft material with a standard Poisson's ratio $\nu = 0.20$. The mechanical response obtained with continuum elements is compared with the one obtained with a RBSM, in particular for the elastic (or quasi-) isotropic response for the uni-axial $\mathbf{H}_{11}$ and deviatoric deformation $\mathbf{H}_D$ modes.

3.1 Soft and auxetic microstructure

From the HM model (Eq. 5) and to guarantee that all bonds have a semi-positive stiffness, it is observed that $k_c = [0, G]$ for an auxetic response. It is also evidenced that the range of possible Poisson's ratios depends on k_c and is conditioned by both the magenta and red bonds:

$$k_c \in \ ]0, G] \ \rightarrow \ \nu^{\mathsf{PS}} \in \left[\ \tfrac{k_c - G}{k_c + G} \ , \ \tfrac{k_c}{2G + k_c}\ \right] \tag{6}$$

in which $\nu^{\mathsf{PS}} = [-1, 0]$ for the particular case $k_c = 0$, meaning that only very soft auxetic materials can be reproduced or, as limit case, a material with null Poisson's ratio. Therefore, the assigned topology requires that $k_c = 0$ and $k_r = 0$, for which the green bonds have the maximum stiffness. The FE model is depicted in Fig. 1b, for which is evidenced that bonds have a cell-type shape to reach the desired low stiffness values required for a soft material. A shear modulus of the material used in the printing process is considered to be given as $G_{print} = 100G$.

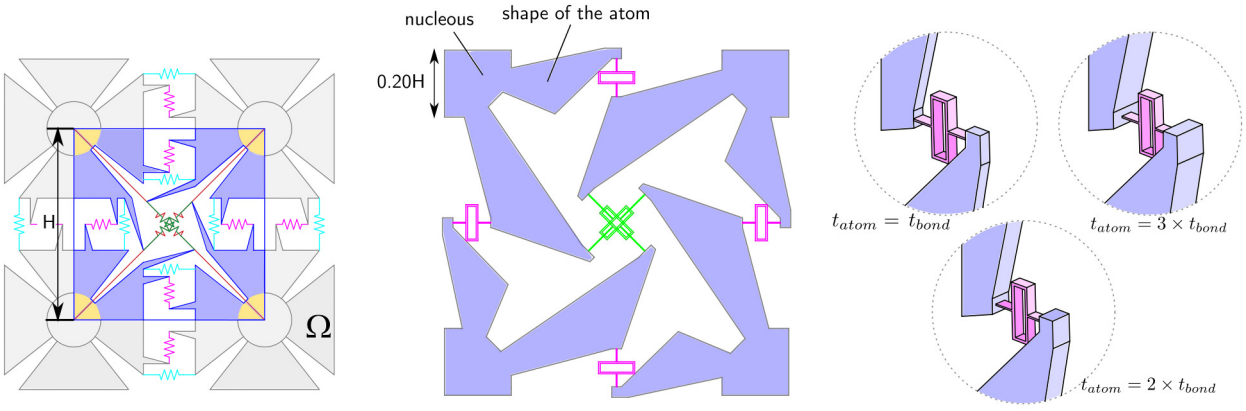

(a) Rigid Body Spring Model (RBSM) (b) Designed topology (c) Considered thicknesses for the atoms

Figure 1: HM internal structure to reach an elastic quasi-isotropic response with a Poisson's ratio $\approx \nu = -1.0$.

3.2 Soft microstructure with positive Poisson's ratio

The design of the microstructure for a soft material with $\nu = 0.2$ is here conducted. To limit the number of bonds, it has been assumed a value for $k_c = \frac{G}{2}$ such that the shear-type bonds have a null stiffness ($k_m = 0$).

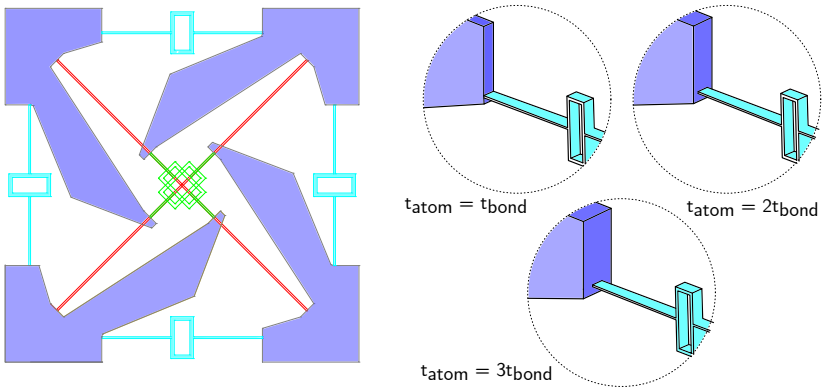

Figure 2: HM internal structure to reach an elastic quasi-isotropic response with a Poisson's ratio $\approx \nu = 0.20$.

4 DISCUSSION OF RESULTS AND FINAL REMARKS

The performance in terms of isotropy is evaluated from the energy ratio $\mathcal{U}(\alpha)/\mathcal{U}(0)$ for both uni-axial $\mathbf{H}_{11}$ and deviatoric $\mathbf{H}_{\mathsf{D}}$ deformation modes. Concerning the auxetic material, the higher deviations found are 35% for $\mathbf{H}_{11}$ and 26% for $\mathbf{H}_{\mathsf{D}}$ and are associated with the HM whose atoms and bonds have the same thickness. In the case of an atom with a thickness that is three times larger than the bonds (three layers), the deviations of the isotropy ratio are of 13% and 11.5% for $\mathbf{H}_{11}$ and $\mathbf{H}_{\mathsf{D}}$, respectively. When the atom is rigid, the deviations are negligible as presented in Fig. 3.

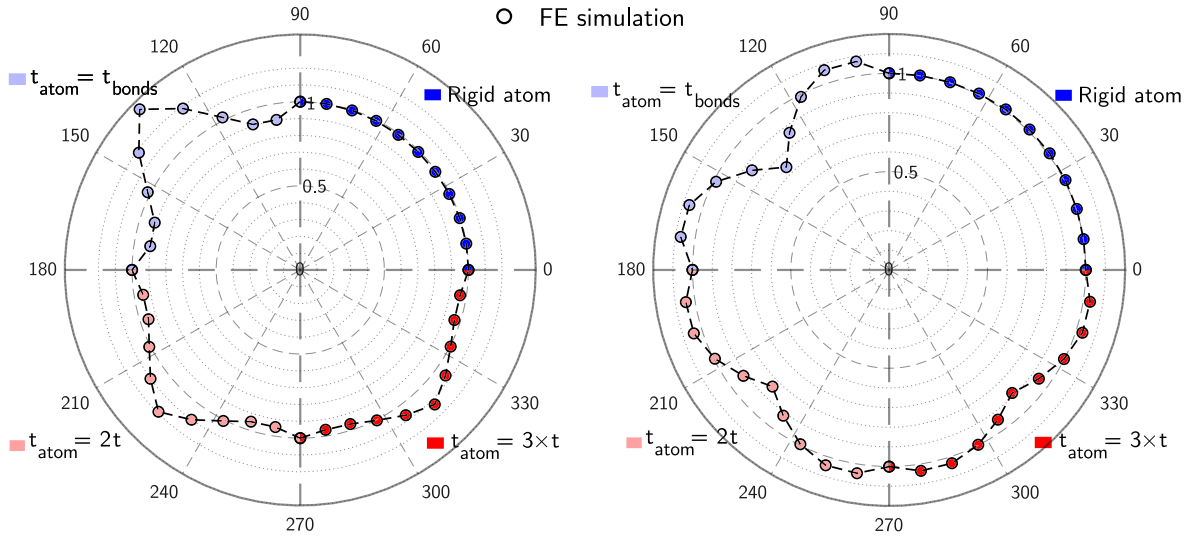

(a) Uni-axial deformation mode, $\mathbf{H}_{11}$

(b) Deviatoric deformation mode, $\mathbf{H}_{\mathrm{D}}$

Figure 3: Elastic isotropy ratio $\mathcal{U}(\alpha)/\mathcal{U}(0)$ of the HM under PS conditions for the soft material with $\nu = -1.0$.

To what concerns the material with a standard Poisson's ratio ($\nu = 0.2$), the higher deviations for the isotropy ratio are also found when the atom has the same thickness of the bonds, and range from 15% for $\mathbf{H}_{11}$ to 30% for $\mathbf{H}_{\mathrm{D}}$. When atoms have a thickness that is three times larger than the thickness of bonds (three layers), the isotropy ratio deviations are 9% and 20% for $\mathbf{H}_{11}$ and $\mathbf{H}_{\mathrm{D}}$, respectively. When the atom is rigid, the deviations are again negligible as presented in Fig. 4.

The results demonstrate that the loss of isotropy is mainly related with the deformability of the atoms. When atoms are rigid and for both the designed microstructures, the isotropy ratio is close to 1.0 and is in agreement with the results predicted through the heuristic molecule according to a Rigid-Body-spring-model [12]. It is also important to remark that the isotropy ratio is also influenced by the shear and the bending stiffness terms of the bonds, i.e. the bond connection with the atoms. Differently from a pure spring-based link, in which only a line stiffness is provided for bonds, a continuum-based modelling leads to shear and bending stiffness that depend on the slenderness ratio of the link. Such influence is especially observed for the auxetic $\nu = -1.0$ microstructure, as bonds with lower slenderness ratio have been adopted. As a consequence, the isotropy curves have, for all the HMs with deformable atoms, a lobed shape. A different behaviour is found for the soft HM with a $\nu = 0.2$ since the influence of the latter undesired stiffness terms gives a lower contribution with respect to the axial stiffness. Such effect can be mathematically demonstrated, however, this is outside the scope of this communication.

5 CONCLUSIONS

The design of the microstructure for an auxetic material ($\nu = -1.0$) and a standard material ($\nu = 0.2$) is presented and assuming the same value of macroscopic shear modulus ($G = 5$ MPa), despite the use of a standard printing material. The design is based on a planar molecular model

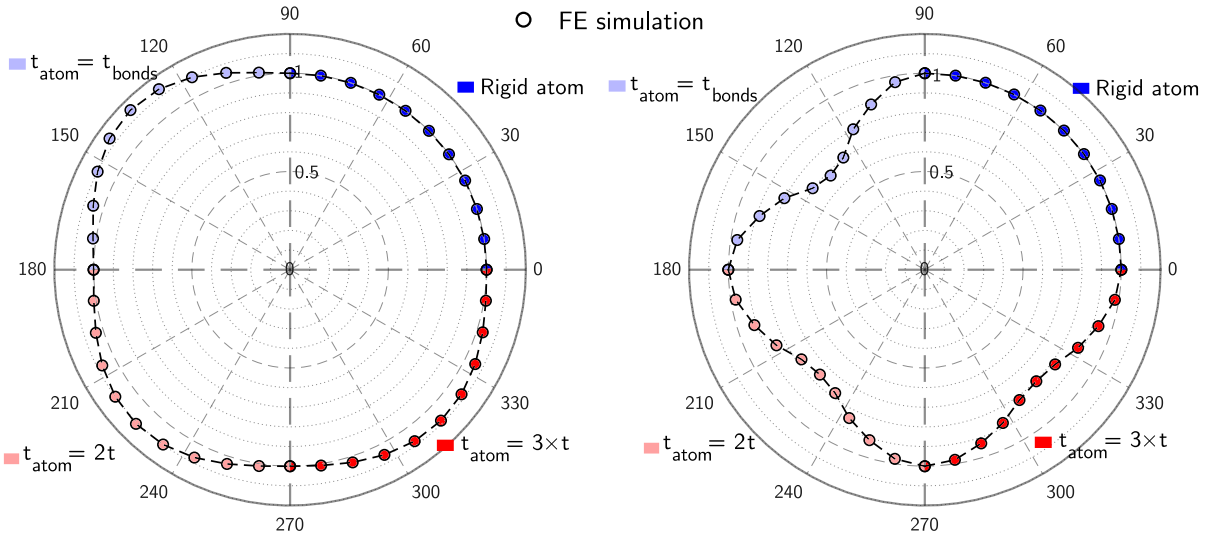

(a) Uni-axial deformation mode, $\mathbf{H_{11}}$

(b) Deviatoric deformation mode, $\mathbf{H_D}$

Figure 4: Elastic isotropy ratio $\mathcal{U}(\alpha)/\mathcal{U}(0)$ of the HM under PS conditions for the soft material with $\nu = 0.2$.

whose unit-cell derives from a RBSM heuristic molecule (HM) composed of shaped atoms with both centered and non-centered bond ligaments. A homogenization approach is employed to establish a relationship between the stiffness of bonds and the macroscopic elastic properties of the desired isotropic Cosserat material.

The practical significance of the HM for additive manufacturing purposes lies in: (i) the modelling of the HM through a continuum-based Finite Element model, and (ii) in the constitutive description of the atoms and bonds, which is determined based on the elastic properties of the material used in the printing process, combined with the shape of the connections (bonds).

Results demonstrate a good match with the expected properties in terms of elastic isotropic response when compared to a RBSM approach, especially for the microstructures with less deformable atoms. The latter has been achieved by increasing the thickness of the atoms t_{atom} in respect to the thickness of the bonds t_{bond} since a single material is envisaged for the printing process. Nonetheless, a lower deformability for atoms can be also achieved through a multi-material printing process [1] and, therefore, by adopting $t_{atom} = t_{bond}$. It has been also observed that the adoption of a continuum-based approach for bonds leads to spurious shear and bending (in the local reference of the bond) stiffness terms at the connection bond-atom, which can be reduced by (1) changing the geometry of these linking parts by increasing its slenderness ratio, or eliminated by (2) changing the bonds-atom joints through hinged connectors. Although the first solution can be impractical if the geometric dimensions are significantly reduced, the second solution can be achieved as addressed in [14] even within a non-assembly (i.e. monolithic) additive manufacturing paradigm.

6 ACKNOWLEDGEMENTS

The first author gratefully acknowledges the funding of the Ministry of University and Research, MUR, Italy, within the program PON Research and Innovation 2014-2020, and research project code (CUP) D45F21003530001: *'Multiphysics of innovative microstructured materials with adaptive mechanical properties for the safety and optimal performance of constructions'*.

References

[1] A. Mitchell, U. Lafont, M. Hołyńska, C. Semprimoschnig, Additive manufacturing — a review of 4d printing and future applications, Additive Manufacturing 24 (2018) 606–626. doi:https://doi.org/10.1016/j.addma.2018.10.038.
URL https://www.sciencedirect.com/science/article/pii/S2214860417304013

[2] M. Wallbanks, M. F. Khan, M. Bodaghi, A. Triantaphyllou, A. Serjouei, On the design workflow of auxetic metamaterials for structural applications, Smart Materials and Structures 31 (2) (2021) 023002. doi:10.1088/1361-665X/ac3f78.
URL https://dx.doi.org/10.1088/1361-665X/ac3f78

[3] J. B. Choi, R. S. Lakes, Non-linear properties of metallic cellular materials with a negative Poisson's ratio, Journal of Materials Science 27 (19) (1992) 5375–5381. doi:10.1007/BF02403846.
URL https://doi.org/10.1007/BF02403846

[4] I. I. Argatov, R. Guinovart-Díaz, F. J. Sabina, On local indentation and impact compliance of isotropic auxetic materials from the continuum mechanics viewpoint, International Journal of Engineering Science 54 (2012) 42–57. doi:https://doi.org/10.1016/j.ijengsci.2012.01.010.
URL https://www.sciencedirect.com/science/article/pii/S0020722512000213

[5] J. B. Choi, R. S. Lakes, Fracture toughness of re-entrant foam materials with a negative Poisson's ratio: experiment and analysis, International Journal of Fracture 80 (1) (1996) 73–83. doi:10.1007/BF00036481.
URL https://doi.org/10.1007/BF00036481

[6] A. Alderson, J. Rasburn, S. Ameer-Beg, P. G. Mullarkey, W. Perrie, K. E. Evans, An Auxetic Filter: A Tuneable Filter Displaying Enhanced Size Selectivity or Defouling Properties, Industrial Engineering Chemistry Research 39 (3) (2000) 654–665. doi:10.1021/ie990572w.
URL https://doi.org/10.1021/ie990572w

[7] G. Imbalzano, P. Tran, T. D. Ngo, P. V. Lee, A numerical study of auxetic composite panels under blast loadings, Composite Structures 135 (2016) 339–352. doi:https://doi.org/10.1016/j.compstruct.2015.09.038.
URL https://www.sciencedirect.com/science/article/pii/S0263822315008843

[8] K. H. Matlack, M. Serra-Garcia, A. Palermo, S. D. Huber, C. Daraio, Designing perturbative metamaterials from discrete models, Nature Materials 17 (4) (2018) 323–328.

doi:10.1038/s41563-017-0003-3.
URL https://doi.org/10.1038/s41563-017-0003-3

[9] K. Wang, Y. Chen, M. Kadic, C. Wang, M. Wegener, Nonlocal interaction engineering of 2D roton-like dispersion relations in acoustic and mechanical metamaterials, Communications Materials 3 (1) (2022) 35. doi:10.1038/s43246-022-00257-z.
URL https://doi.org/10.1038/s43246-022-00257-z

[10] Y. Zhang, B. Li, Q. S. Zheng, G. M. Genin, C. Q. Chen, Programmable and robust static topological solitons in mechanical metamaterials, Nature Communications 10 (1) (2019) 5605. doi:10.1038/s41467-019-13546-y.
URL https://doi.org/10.1038/s41467-019-13546-y

[11] S. Casolo, A linear-elastic heuristic-molecular modelling for plane isotropic micropolar and auxetic materials, International Journal of Solids and Structures 224 (111042) (2021). doi:10.1016/j.ijsolstr.2021.111042.

[12] L. C. da Silva, N. Grillanda, S. Casolo, Heuristic molecular modelling of quasi-isotropic auxetic metamaterials under large deformations, International Journal of Mechanical Sciences 251 (2023) 108316. doi:https://doi.org/10.1016/j.ijmecsci.2023.108316.
URL https://www.sciencedirect.com/science/article/pii/S0020740323002187

[13] V. Diana, Anisotropic Continuum-Molecular Models: A Unified Framework Based on Pair Potentials for Elasticity, Fracture and Diffusion-Type Problems, Archives of Computational Methods in Engineering 30 (2) (2023) 1305–1344. doi:10.1007/s11831-022-09846-0.
URL https://doi.org/10.1007/s11831-022-09846-0

[14] J. S. Cuellar, G. Smit, D. Plettenburg, A. Zadpoor, Additive manufacturing of non-assembly mechanisms, Additive Manufacturing 21 (2018) 150–158. doi:https://doi.org/10.1016/j.addma.2018.02.004.
URL https://www.sciencedirect.com/science/article/pii/S2214860417302130